Leveraging Structures in Fault Diagnosis for Lithium-Ion Battery Packs

Amir Farakhor Dept. of Mechanical Engineering University of Kansas Lawrence, USA a.farakhor@ku.edu

Di Wu Richland, USA di.wu@pnnl.gov

Yebin Wang Pacific Northwest National Laboratory Mitsubishi Electric Research Laboratories Cambridge, USA yebinwang@merl.com

Huazhen Fang Dept. of Mechanical Engineering University of Kansas Lawrence, USA fang@ku.edu

Abstract-Lithium-ion battery packs consist of a varying number of single cells, designed to meet specific application requirements for output voltage and capacity. Effective fault diagnosis in these battery packs is an essential prerequisite for ensuring their safe and reliable operation. To address this need, we introduce a novel model-based fault diagnosis approach. Our approach distinguishes itself by leveraging informative structural properties inherent in battery packs such as uniformity among the constituent cells, and sparsity of fault occurrences to enhance its fault diagnosis capabilities. The proposed approach formulates a moving horizon estimation (MHE) problem, incorporating such structural information to estimate different fault signalsspecifically, internal short circuits, external short circuits, and voltage and current sensors faults. We conduct various simulations to evaluate the performance of the proposed approach under different fault types and magnitudes. The obtained results validate the proposed approach and promise effective fault diagnosis for battery packs.

Index Terms—battery systems, fault diagnosis, moving horizon estimation

I. INTRODUCTION

Lithium-ion battery packs have emerged as an effective solution for energy storage across various applications. Beginning with their use in small portable devices, these battery packs are continuously expanding their role in transportation electrification, including electric aircraft, and in integration of renewable energy through grid energy storage [1, 2]. Despite the advantages of lithium-ion batteries, such as high energy density and long lifespan, they are susceptible to safety risks [3]. This necessitates careful monitoring within their battery management systems to ensure their safe and reliable operation, especially in safety-critical applications. Consequently, fault diagnosis is of utmost importance to lithium-ion battery

Fault diagnosis of lithium-ion battery packs has attracted much attention from both researchers and practitioners. Existing studies can be broadly classified into two categories: 1) model-based approaches [5], and 2) data-driven approaches [6]. Model-based approaches utilize a system model to identify fault occurrences by aligning measurements with model predictions. On the other hand, data-driven approaches involve training a classifier to differentiate between normal and faulty operating conditions. This paper specifically focuses on the development of a model-based approach for fault diagnosis. We thus narrow the subsequent review to model-based approaches.

Recently, model-based fault diagnostics have become the mainstream approach for lithium-ion battery packs. This is mainly due to the advancements in our in-depth understanding of their dynamics. One area of research focuses on sensor fault detection and identification. For instance, the work in [7] solely concentrates on voltage sensor faults in a single battery cell. The study in [8] investigates voltage and current sensor fault diagnosis in a serial-connected battery pack, while [9] introduces a more comprehensive method for sensor fault detection in both serial and parallel-connected battery packs. Another body of research investigates cell fault detection and identification. For example, the study in [10] aims to detect short circuits in serial-connected battery packs. Additionally, the works in [7, 11] develop fault detection approaches for minor internal short circuits. While many studies focus exclusively on either sensor or cell faults, there are comprehensive approaches in the literature that simultaneously address both types. For instance, the works in [12–14] present fault detection approaches that encompass both sensor and cell faults simultaneously. However, it is worth noting that these studies often rely on a high number of sensors.

Existing fault detection approaches usually require many sensors to capture faults successfully, counter to the practical need for economy in sensor utilization. This paper, however, proposes that we can harness some structural properties inherent in battery packs to enable fault detection with fewer sensors. For instance, exploiting the uniformity of identical cells within the battery pack can significantly enhance fault detection. Additionally, recognizing the distinct nature and severity of various fault types, in conjunction with the low

probability of simultaneous occurrence, raises the question of how such information can be effectively leveraged to improve fault diagnosis. Further, our approach can accommodate sensor faults, in contrast to various studies assuming faultless sensors.

Compared to the existing literature, this paper makes two significant contributions. Firstly, the proposed fault diagnosis approach leverages the structural properties of battery packs, including uniformity among constituent cells, severity of different fault types, and sparsity of fault occurrences. We specifically aim to reduce our reliance on sensor measurements and exploit these structural properties to enhance fault diagnosis capabilities. Secondly, our approach formulates a moving horizon estimation (MHE) problem to integrate structural properties into fault diagnosis. To the best of our knowledge, this study is the first to explore the application of MHE for diagnosing faults in battery packs. The MHE-based formulation enables us to incorporate structural properties for estimating fault signals.

The rest of the paper is outlined as follows. Section II will introduce the battery pack under study and its fault modeling. In Section III, the proposed MHE-based fault diagnosis approach will be presented. Section IV will present simulation results for validation, and we will conclude the paper in Section V.

II. BATTERY PACK AND FAULT MODELING

This section introduces the considered faults for battery packs and subsequently addresses the electro-thermal modeling in the presence of these faults. Battery packs are susceptible to various malfunctions, including cell internal short circuits, external short circuits, sensor faults, resistance increases due to connection looseness, and rapid cell aging [15]. While all faults can impact the performance, internal and external short circuits, along with sensor faults, are particularly severe. Short circuits can induce rapid temperature increases, leading to thermal runaways. Sensor faults can result in overcharging/discharging, significantly affecting cell performance. In this paper, our specific focus centers on 1) cell-level soft internal short circuits, characterized by small incremental currents with limited heat generation occurring in the early stages of internal short circuits; 2) external short circuits; and 3) voltage/current sensor faults. Next, we discuss the battery pack modeling with consideration of these efforts.

Fig. 1 illustrates the circuit structure of a battery module, comprising n battery cells in parallel. The module is equipped with voltage, current, and temperature sensors. Note that such modules can be serially connected to construct larger battery packs with higher output voltage. Nevertheless, we focus on the fault diagnosis of a single module in this paper.

To begin with the electrical model, we employ the Rint model to describe the electrical behavior of the cells, as depicted in Fig. 2 (a). The Rint model encompasses an open-circuit voltage source (OCV) and an internal resistance R_j [16]. To account for internal short circuits, we introduce an additional resistor $R_{\rm ISC,\it j}$ to represent and capture the occur-

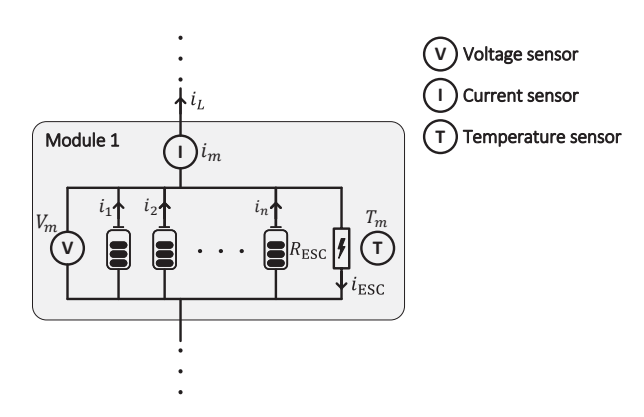


Fig. 1: The considered parallel-series battery pack.

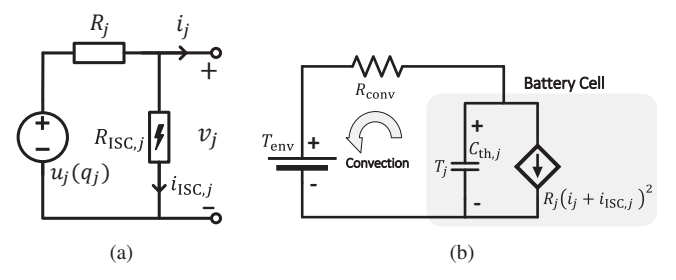


Fig. 2: The cell-level electro-thermal model. (a) The electrical model of the module j. (b) The thermal model of the cell j.

rences within the cells. For cell j, the governing equations are as follows:

$$\dot{q}_{j}(t) = -\frac{1}{Q_{j}} \left(i_{j}(t) + i_{\text{ISC},j}(t) \right),$$
 (1a)

$$v_j(t) = u_j(q_j(t)) - R_j(i_j(t) + i_{ISC,j}(t)),$$
 (1b)

where q_j , Q_j , u_j , v_j , and i_j are the cell's state-of-charge (SoC), capacity, OCV, terminal voltage, and charging/discharging current, respectively. The term $i_{\mathrm{ISC},j}$ denotes the internal short circuit current. We also consider a linear SoC/OCV relationship as follows:

$$u_j(q_j(t)) = \alpha_j + \beta_j q_j(t), \qquad (2)$$

where α_j and β_j are the intercept and slope coefficients of the line.

The thermal behavior of the battery cells is characterized through a lumped capacitance model, illustrated in Fig. 2 (b). This model considers internal power losses as the primary source of heat generation, with heat dissipating through convection to the environment. The governing thermal dynamics are given as follows:

$$C_{\text{th}}\dot{T}_{j}(t) = R_{j} (i_{j}(t) + i_{\text{ISC},j}(t))^{2} - (T_{j}(t) - T_{\text{env}})/R_{\text{conv}},$$
 (3)

where T_j and $T_{\rm env}$ are the temperature of cell j and the environmental temperature, respectively. Further, $C_{\rm th}$ and $R_{\rm conv}$ are the heat capacity and the convective thermal resistance between cell j and the environment, respectively. Note that $i_{\rm ISC},j$ contributes as a heat generation term in the thermal model.

We now shift our attention to external short circuit modeling. This fault is represented by a resistance $R_{\rm ESC}$ in parallel with the module, as illustrated in Fig. 1. By Kirchoff's current law, we have:

$$i_1 + i_2 + \dots + i_n = i_L + i_{ESC},$$
 (4)

where i_L and i_{ESC} are the applied current to the module and the external short circuit current, respectively.

As we explained earlier, each module is equipped with three sensors for voltage, current, and temperature measurements. The voltage sensor measures the voltage across the parallel-connected cells as follows:

$$V_m = v_1 + f_v, (5$$

where V_m is the measured voltage and f_v denotes the sensor fault signal ($f_v \neq 0$ indicates a failed sensor). Also note that $v_1 = v_2 = \cdots = v_n$ since the cells are parallel-connected. The current sensor also measures the applied current to the module as follows:

$$i_m = i_L + f_i, (6$$

where f_i is the current sensor fault signal. The module's temperature is also monitored through a temperature sensor. Here, we assume a uniform temperature distribution among the cells, i.e.,

$$T_m = T_1 = \dots = T_n, \tag{7}$$

where T_m is the measured temperature. Additionally, it is important to note that we do not account for temperature sensor faults in this study. In what follows, we will utilize the presented electro-thermal model in conjunction with the identified faults to formulate the proposed model-based fault diagnosis approach.

III. THE PROPOSED FAULT DIAGNOSIS APPROACH

The central idea of this paper is to investigate the utilization of specific structural properties for the fault diagnosis of battery packs. We specifically focus on integrating the following information into our fault diagnosis approach:

- Sparsity of fault occurrences: A battery pack may be subject to various fault types, but at any given time, only a few faults are likely to occur. This suggests that fault occurrences should be sparse. Although one fault may lead to others over time, sparsity will help us detect the initial fault in the early stages.
- 2) Uniformity among identical constituent cells: Battery packs consist of almost identical cells arranged in series and parallel to meet specific output requirements. It is reasonable to anticipate that cells should exhibit consistent behavior. Deviations in the behavior of a single cell compared to others may indicate a malfunction, such as an internal short circuit. Therefore, we exploit the fact that constituent cells are identical and impose a maximum discrepancy threshold among them. Any deviation beyond the predefined threshold can be utilized to detect and identify faults.

3) Severity of various fault types: It is important to acknowledge that distinct fault types have varying impacts on battery packs. Let us, for instance, compare an internal short circuit fault with an external one. An internal short circuit primarily affects individual cells within a battery pack. Characterized by a minor short circuit current, detecting and identifying faults becomes challenging due to its limited impact on overall performance. In contrast, external short circuits have the potential to affect more than a single cell—potentially the entire module—with a substantial impact and high short circuit current. Incorporating these characteristics of different fault types will enhance the accuracy in fault diagnosis.

For the battery pack in Fig. 1, we formulate an MHE problem for estimating fault signals while leveraging the structural properties mentioned above. First introduced in [17], MHE is a method that employs the most recent measurements within a time window to estimate unknown states. This method finds application in tasks such as state estimation, fault detection, and disturbance estimation. MHE formulates the estimation as an optimization problem that enables possible incorporation of further constraints on estimated variables.

To begin with, we discretize the system dynamics in (2) and (3) through the forward Euler method. We will also adopt the convention of using bold lowercase and uppercase letters for vectors and matrices, respectively. Subsequently, we compactly represent the system dynamics and measurement models as follows:

$$x[k+1] = g(x[k], u[k], f_{ISC}[k]) + w_x[k],$$
 (8a)

$$y[k] = h(x[k], u[k], f_{ESC}[k], f_{v,i}[k]) + w_{u}[k],$$
 (8b)

where x, u, y are the states, inputs, and measurements, respectively; $f_{\rm ISC}$, $f_{\rm ESC}$, and $f_{v,i}$ are the internal short circuit, external short circuit, and sensor fault signals, respectively. These variables are specified as follows:

$$oldsymbol{x} = egin{bmatrix} q_1 \ dots \ q_n \ T_1 \ dots \ T_n \end{bmatrix}, \; oldsymbol{y} = egin{bmatrix} V_m \ i_m \ T_m \end{bmatrix}, \; oldsymbol{u} = egin{bmatrix} i_1 \ dots \ i_n \end{bmatrix}, \; oldsymbol{f}_{ ext{ISC},n} \end{bmatrix}, \ oldsymbol{f}_{ ext{ISC},n} \end{bmatrix}, \ oldsymbol{f}_{ ext{v},i} = egin{bmatrix} f_v \ f_i \end{bmatrix}, \; f_{ ext{ESC}} = i_{ ext{ESC}}. \ \end{pmatrix}$$

The terms $w_x \in \mathbb{R}^{2n}$ and $w_y \in \mathbb{R}^3$ are also the bounded process and measurement disturbances, respectively.

Proceeding forward, we focus on the formulation of a cost function for the MHE problem. Our design aims to promote the sparsity of fault occurrences within our fault diagnosis approach. To achieve this objective, we introduce an ℓ_0 -

norm regularization term into the cost function of the MHE framework as follows:

$$\phi[k] = \sum_{t=k-H}^{k-1} \|\boldsymbol{w}_{x}[t]\|_{\boldsymbol{Q}}^{2} + \|\boldsymbol{w}_{y}[t]\|_{\boldsymbol{R}}^{2} + \|\boldsymbol{F}[t]\|_{0} + \|\Delta\boldsymbol{F}[t]\|_{0} + \|\boldsymbol{w}_{y}[k]\|_{\boldsymbol{R}}^{2} + \phi_{ac}\left(\hat{\boldsymbol{x}}[k-H]\right),$$
(9)

where $\boldsymbol{F} = [f_{\text{ISC}}^{\top} f_{\text{ESC}} f_{v,i}^{\top}]^{\top}$ is the concatenated fault vector and $\|\cdot\|_0$ denotes its ℓ_0 -norm; $\Delta \boldsymbol{F}$ is the incremental changes in the fault signals defined as

$$\Delta \boldsymbol{F}[k] = \boldsymbol{F}[k] - \boldsymbol{F}[k-1]. \tag{10}$$

Further, H is the horizon length, Q and R are weight matrices, and $\hat{x}[k-H]$ is the estimated x at time step k-H. In addition, $\phi_{\rm ac}\left(\hat{x}[k-H]\right)$ denotes the arrival cost. The arrival cost represents an estimation of the initial condition, encompassing prior information beyond the horizon window, from time t=0 to t=k-H.

Note that the inclusion of the ℓ_0 -norm in (9) renders the cost function nondifferentiable and the underlying optimization problem non-convex, making the solution computationally demanding [18]. To make the problem tractable, we introduce a relaxation of the ℓ_0 -norm using a mixed $\ell_{2,1}$ -norm as follows:

$$\|\boldsymbol{F}\|_{2,1} = \left\| \begin{bmatrix} \lambda_{\text{ISC}} \|\boldsymbol{f}_{\text{ISC}}\|_2 \\ \lambda_{\text{ESC}} \|\boldsymbol{f}_{\text{ESC}}\|_2 \\ \lambda_{v,i} \|\boldsymbol{f}_{v,i}\|_2 \end{bmatrix} \right\|_1, \tag{11}$$

where $\lambda_{\rm ISC}$, $\lambda_{\rm ESC}$, and $\lambda_{v,i}$ are the respective weights for each fault type [19, 20]. Further, $\|\cdot\|_1$ and $\|\cdot\|_2$ denote the ℓ_1 and ℓ_2 -norm operators and $\|\cdot\|_Q^2 = (\cdot)^\top Q(\cdot)$. The motivation behind the design in (11) is twofold. First, we aim to promote sparsity among different fault types. Practically, the occurrence of multiple fault types simultaneously is improbable, and the promotion of sparsity can be fine-tuned through the respective weights assigned to each fault type. Secondly, by incorporating the ℓ_2 -norm of each fault type, we effectively penalize fault signals within each category, thereby promoting sparsity at a lower level. We also relax the ℓ_0 -norm of ΔF in (9) with its ℓ_2 -norm and subsequently express the cost function for the MHE problem as follows:

$$\phi[k] = \phi_{ac} \left(\hat{x}[k-H] \right) + \sum_{t=k-H}^{k-1} \| \boldsymbol{w}_x[t] \|_{\boldsymbol{Q}}^2 + \| \boldsymbol{w}_y[t] \|_{\boldsymbol{R}}^2$$

$$+ \| \boldsymbol{w}_y[k] \|_{\boldsymbol{R}}^2 + \sum_{t=k-H}^{k-1} \| \Delta \boldsymbol{F}[t] \|_{\boldsymbol{P}}^2 + \| \boldsymbol{F}[t] \|_{2,1}^2 ,$$
(12)

where P is a weight matrix. Having laid out the cost function of the MHE problem, we can now shift our focus to the constraints.

We have addressed fault sparsity by penalizing signals in the cost function and will further consider uniformity among cells and fault severity through additional constraints. We apply constraints to leverage the uniformity among identical constituent cells, as follows:

$$|q_{j+1} - q_j| \le \Delta q,\tag{13a}$$

$$|T_{j+1} - T_j| \le \Delta T,\tag{13b}$$

where Δq and ΔT are the pre-specified thresholds. These constraints mirror the consistent behavior expected from individual cells within a battery pack. Note that we only impose constraints on adjacent cells in a parallel-connected module to enforce the uniformity with a small number of inequalities. To distinguish between the severity of different fault types, we further introduce upper and lower limits on the magnitude of the fault signals as follows:

$$f_{\rm ISC}^{\rm min} \le f_{\rm ISC} \le f_{\rm ISC}^{\rm max},$$
 (14a)

$$f_{\rm ESC}^{\rm min} \le f_{\rm ESC} \le f_{\rm ESC}^{\rm max},$$
 (14b)

$$\boldsymbol{f}_{v,i}^{\min} \le \boldsymbol{f}_{v,i} \le \boldsymbol{f}_{v,i}^{\max}, \tag{14c}$$

where $f^{\text{max/min}}$ denotes the upper/lower bound of each fault type. Similar upper and lower bounds are also introduced for noise signals to differentiate them from faults. These constraints are also expressed as follows:

$$\boldsymbol{w}_{x}^{\min} \le \boldsymbol{w}_{x} \le \boldsymbol{w}_{x}^{\max},\tag{15a}$$

$$\boldsymbol{w}_{\boldsymbol{y}}^{\min} \leq \boldsymbol{w}_{\boldsymbol{y}} \leq \boldsymbol{w}_{\boldsymbol{y}}^{\max}. \tag{15b}$$

We are now ready to formulate the MHE problem for our fault diagnosis approach. The MHE problem is expressed as follows:

$$\begin{split} \text{minimize} \quad & \ell_{\text{ac}}\left(\hat{\boldsymbol{x}}[k-H]\right) + \sum_{t=k-H}^{k-1} \left\|\boldsymbol{w}_{x}[t]\right\|_{\boldsymbol{Q}}^{2} + \left\|\boldsymbol{w}_{y}[t]\right\|_{\boldsymbol{R}}^{2} \\ & + \left\|\boldsymbol{w}_{y}[k]\right\|_{\boldsymbol{R}}^{2} + \sum_{t=k-H}^{k-1} \left\|\Delta \boldsymbol{F}[t]\right\|_{\boldsymbol{P}}^{2} + \left\|\boldsymbol{F}[t]\right\|_{2,1}^{2}, \end{split}$$

SoC dynamics:

$$q_j[t+1] = q_j[t] - \frac{\Delta t}{Q_j} \left(i_j[k] + i_{\mathrm{ISC},j}[k] \right), \label{eq:qj}$$

Temperature dynamics:

$$T_{j}[t+1] = T_{j}[t] + \frac{\Delta t}{C_{\text{th}}} \left[R_{j} \left(i_{j}[k] + i_{\text{ISC},j}[k] \right)^{2} - \left(T_{j}[t] - T_{\text{env}} \right) / R_{\text{conv}} \right],$$

Incremental fault dynamics:

$$\mathbf{F}[t+1] = \mathbf{F}[t] + \Delta \mathbf{F}[t+1],$$

Fault and noise constraints:

$$\begin{split} & \boldsymbol{f}_{\text{ISC}}^{\text{min}} \leq \boldsymbol{f}_{\text{ISC}} \leq \boldsymbol{f}_{\text{ISC}}^{\text{max}}, \ \boldsymbol{f}_{\text{ESC}}^{\text{min}} \leq \boldsymbol{f}_{\text{ESC}} \leq \boldsymbol{f}_{\text{ESC}}^{\text{max}}, \\ & \boldsymbol{f}_{v,i}^{\text{min}} \leq \boldsymbol{f}_{v,i} \leq \boldsymbol{f}_{v,i}^{\text{max}}, \\ & \boldsymbol{w}_{x}^{\text{min}} \leq \boldsymbol{w}_{x} \leq \boldsymbol{w}_{x}^{\text{max}}, \ \boldsymbol{w}_{y}^{\text{min}} \leq \boldsymbol{w}_{y} \leq \boldsymbol{w}_{y}^{\text{max}}, \end{split}$$

Balancing constraints:

$$|q_{j+1} - q_j| \le \Delta q,$$

$$|T_{j+1} - T_j| \le \Delta T,$$
(16)

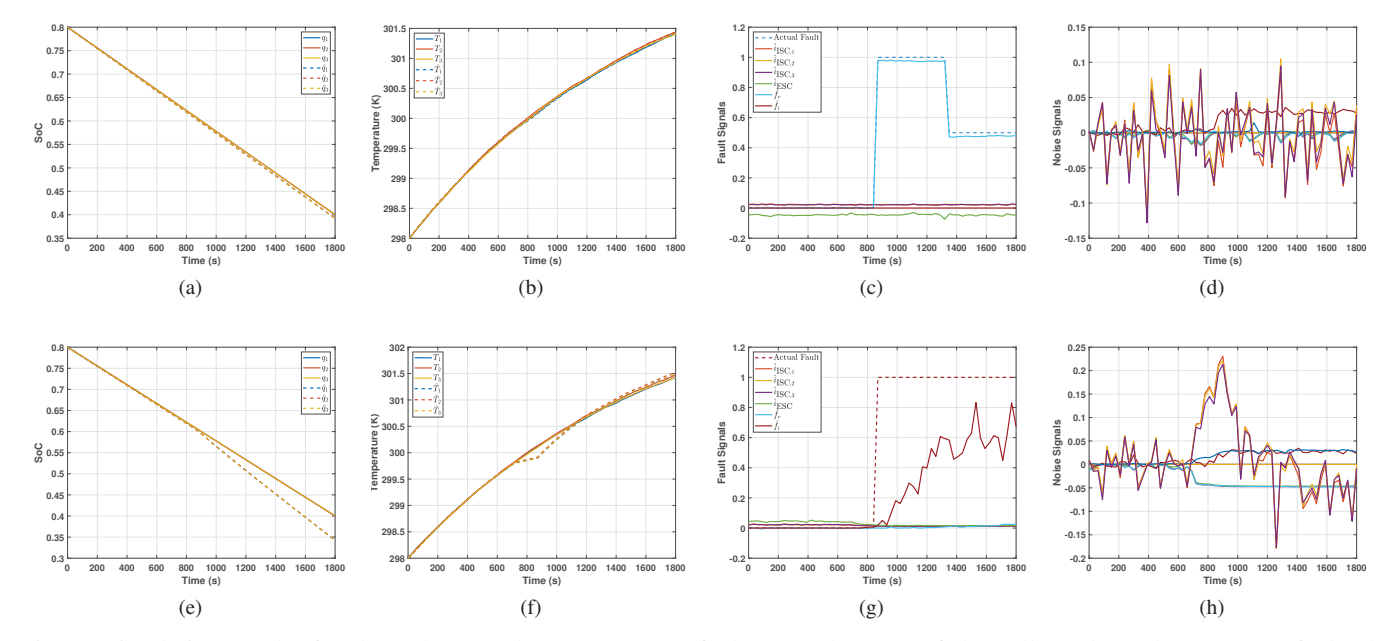


Fig. 3: Simulation results for the voltage and current sensor faults. (a) The SoC of the cells under voltage sensor fault. (b) The temperature of the cells under voltage sensor fault. (c) The estimated fault signals under voltage sensor fault. (d) The estimated noise signals under voltage sensor fault. (e) The SoC of the cells under current sensor fault. (f) The temperature of the cells under current sensor fault. (g) The estimated fault signals under current sensor fault. (h) The estimated noise signals under current sensor fault.

where Δt is the sampling time. While fully characterizing the arrival cost poses challenges, literature has explored various techniques for its estimation. One approach involves employing an unconstrained probabilistic estimation method, such as Kalman filtering, before optimizing the problem, followed by imposing a penalty on the discrepancy between the current and previous estimates. In this study, we specifically employ the approach in [21] using an extended Kalman filter. Overall, the optimization problem in (16) effectively estimates the fault signals while leveraging the inherent structural properties of the battery pack.

IV. SIMULATION RESULTS

In this section, we perform various simulations on a battery pack under different fault conditions to validate the proposed fault diagnosis approach. The considered system is a module, as depicted in Fig. 1, comprising three cells in parallel. The specifications are summarized in Table I. The initial SoC of the cells is set to 0.8, and the module is discharged at a constant current of 6 A. We also assign the parameters in (11), namely $\lambda_{\rm ISC}$, $\lambda_{\rm ESC}$, and $\lambda_{v,i}$, values of 1.5, 1, and 2, respectively. The fmincon package in the Matlab software is used to solve the optimization problem in (16). We initially assess the proposed approach's performance under sensor faults and subsequently shift our focus to short circuit faults.

A. Sensor Faults

Fig. 3 illustrates the simulation results for the sensor faults. Starting with a faultless voltage sensor, a +1 V bias is introduced to the voltage measurement (i.e., $f_v = 1$) at time instant

TABLE I: Specifications of the considered battery pack

Symbol	Parameter	Value [Unit]
\overline{n}	Number of battery cells	3
v	Cell nominal voltage	3.6 [V]
Q	Cell nominal capacity	2.5 [Ah]
R	Cell internal resistance	31.3 [m Ω]
C_{th}	Thermal capacitance	40.23 [J/K]
$R_{\rm conv}$	Convection thermal resistance	41.05 [K/W]
$T_{ m env}$	Environment temperature	298 [K]
Δq	SoC balancing threshold	0.5%
ΔT	Temperature balancing threshold	0.5 [K]
Δt	Sampling time	30 [s]
Н	Horizon length	300 [s]

800 s, and subsequently reduced to 0.5 V at the 1300-second mark. Figs. 3 (a)-(b) present the actual and estimated SoC and temperature values for the cells. The estimation accuracy is high before the occurrence of the voltage sensor fault; however, slight deviations are observed in the SoC estimation performance afterwards. Fig. 3 (c) depicts the estimated fault signals, indicating the successful identification of the voltage sensor fault along with its magnitude. The corresponding noise signals are also illustrated in Fig. 3 (d).

Subsequently, we conduct simulations with a current sensor fault, characterized by a bias of +1 A, starting at time instant

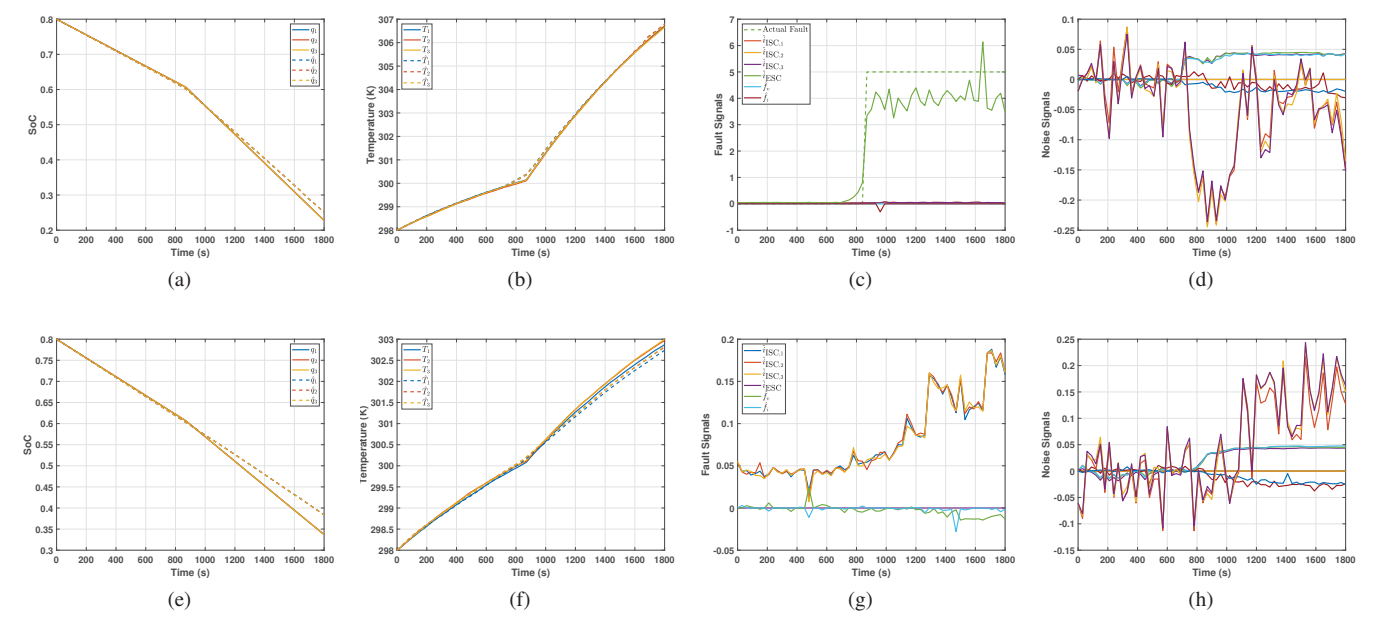


Fig. 4: Simulation results of the internal and external short circuit faults. (a) The SoC of the cells under external short circuit fault. (b) The temperature of the cells under external short circuit fault. (c) The estimated external short circuit fault signal. (d) The estimated noise signals under external short circuit fault. (e) The SoC of the cells under internal short circuit fault. (f) The temperature of the cells under internal short circuit fault. (g) The estimated internal short circuit fault signal. (h) The estimated noise signals under internal short circuit fault.

800 s. Fig. 3 (e) shows the estimated SoC values. It is evident that SoC estimation remains accurate prior to the occurrence of the fault. However, post-fault, the estimation tends to underestimate SoC values due to the measured current exceeding the actual applied current to the module. Fig. 3 (f) further presents the estimated cell temperatures. The estimated fault signals are illustrated in Fig. 3 (g). We observe that our approach effectively detects the fault, although the estimated fault magnitude is not very accurate, and the detection is comparatively slower than that observed for the voltage sensor fault. This is because a faulty current sensor results in inaccurate SoC estimation. Given the slow dynamics of SoC in cells, effective fault detection takes some time. Additionally, it is worth noting that the severity of the current sensor fault correlates with the speed of detection.

B. Short Circuit Faults

We evaluate the efficacy of the proposed approach for internal and external short circuit faults. Figs. 4 (a)-(d) present the obtained results for a 5 A external short circuit fault. In Figs. 3 (a)-(b), the SoC and temperature estimation performances are depicted with good accuracy. Fig. 4 (c) illustrates the estimated fault signals, indicating the successful and quick detection of the fault. This rapid detection is due to the severity of external short circuits, which significantly impacts the module's performance. The corresponding estimated noise signals are also depicted in Fig. 4 (d).

We investigate an internal short circuit on cell 1 by introducing a resistance $R_{\rm ISC,1}=4~\Omega$, starting at time instant 800 s.

Fig. 4 (e) depicts the estimated SoC of the cells. The proposed approach tends to overestimate the SoC values, as the internal short circuit depletes SoC without providing clear indications through sensor measurements. The estimated temperatures of the cells are depicted in Fig. 4 (f) with good precision. The estimated fault signals are illustrated in Fig. 4 (g). We observe that our approach detects internal short circuit faults in all cells in parallel. This implies that while our approach can detect faults, it cannot precisely identify the specific cell affected. The primary reason for this limitation lies in the structural non-differentiation among $R_{\rm ISC,\it j}$ in the presented model. Also note that the detection is not rapid for internal short circuit faults, as we assume minor internal short circuits with minimal effects on the performance of the battery pack.

V. CONCLUSION

The sweeping growth of lithium-ion battery packs in safety-critical applications, such as electric vehicles and aircraft, underscores the need for effective fault diagnosis. This paper addresses this issue by introducing a novel model-based fault diagnosis approach. The proposed approach, at its core, aims to explore how specific structural information—including the different nature and severity of fault types, uniformity among identical constituent cells, and the sparsity of fault occurrences—can be leveraged to enhance fault diagnosis. Our approach enables this central idea by formulating an MHE-based fault diagnosis problem where the structural information is used as constraints and penalization terms. By doing so, we effectively estimate the fault signals with fewer number of

sensors and measurements. The proposed approach also handles multiple fault types of internal and external short circuits and sensor faults. For validation, we conduct various simulations under different fault scenarios. The obtained results are promising in terms of fault detection and identification with a low sensor count.

REFERENCES

- [1] A. W. Schäfer, S. R. Barrett, K. Doyme, L. M. Dray, A. R. Gnadt, R. Self, A. O'Sullivan, A. P. Synodinos, and A. J. Torija, "Technological, economic and environmental prospects of all-electric aircraft," *Nature Energy*, vol. 4, no. 2, pp. 160–166, 2019.
- [2] K. M. Tan, T. S. Babu, V. K. Ramachandaramurthy, P. Kasinathan, S. G. Solanki, and S. K. Raveendran, "Empowering smart grid: A comprehensive review of energy storage technology and application with renewable energy integration," *Journal of Energy Storage*, vol. 39, p. 102591, 2021.
- [3] B. Xu, J. Lee, D. Kwon, L. Kong, and M. Pecht, "Mitigation strategies for li-ion battery thermal runaway: A review," *Renewable and Sustainable Energy Reviews*, vol. 150, p. 111437, 2021.
- [4] R. Xiong, W. Sun, Q. Yu, and F. Sun, "Research progress, challenges and prospects of fault diagnosis on battery system of electric vehicles," *Applied Energy*, vol. 279, p. 115855, 2020.
- [5] X. Hu, K. Zhang, K. Liu, X. Lin, S. Dey, and S. Onori, "Advanced fault diagnosis for lithium-ion battery systems: A review of fault mechanisms, fault features, and diagnosis procedures," *IEEE Industrial Electronics Magazine*, vol. 14, no. 3, pp. 65–91, 2020.
- [6] A. Samanta, S. Chowdhuri, and S. S. Williamson, "Machine learning-based data-driven fault detection/diagnosis of lithium-ion battery: A critical review," *Electronics*, vol. 10, no. 11, 2021.
- [7] R. Yang, R. Xiong, and W. Shen, "On-board diagnosis of soft short circuit fault in lithium-ion battery packs for electric vehicles using an extended kalman filter," *CSEE Journal of Power and Energy Systems*, vol. 8, no. 1, pp. 258–270, 2022.

- [8] R. Xiong, Q. Yu, W. Shen, C. Lin, and F. Sun, "A sensor fault diagnosis method for a lithium-ion battery pack in electric vehicles," *IEEE Transactions on Power Electronics*, vol. 34, no. 10, pp. 9709–9718, 2019.
- [9] C. Zheng, Z. Chen, and D. Huang, "Fault diagnosis of voltage sensor and current sensor for lithium-ion battery pack using hybrid system modeling and unscented particle filter," *Energy*, vol. 191, p. 116504, 2020.
- [10] B. Xia, Y. Shang, T. Nguyen, and C. Mi, "A correlation based fault detection method for short circuits in battery packs," *Journal of Power Sources*, vol. 337, pp. 1–10, 2017.
- [11] X. Kong, Y. Zheng, M. Ouyang, L. Lu, J. Li, and Z. Zhang, "Fault diagnosis and quantitative analysis of micro-short circuits for lithium-ion batteries in battery packs," *Journal of Power Sources*, vol. 395, pp. 358–368, 2018.
- [12] Y. Kang, B. Duan, Z. Zhou, Y. Shang, and C. Zhang, "Online multi-fault detection and diagnosis for battery packs in electric vehicles," *Applied Energy*, vol. 259, p. 114170, 2020.
- [13] K. Zhang, X. Hu, Y. Liu, X. Lin, and W. Liu, "Multi-fault detection and isolation for lithium-ion battery systems," *IEEE Transactions on Power Electronics*, vol. 37, no. 1, pp. 971–989, 2022.
- [14] Y. Cheng, M. D'Arpino, and G. Rizzoni, "Optimal sensor placement for multifault detection and isolation in lithium-ion battery pack," *IEEE Transactions on Transportation Electrification*, vol. 8, no. 4, pp. 4687–4707, 2022.
- [15] R. Bubbico, V. Greco, and C. Menale, "Hazardous scenarios identification for li-ion secondary batteries," *Safety Science*, vol. 108, pp. 72–88, 2018.
- [16] G. L. Plett, Battery management systems, Volume I: Battery modeling. Artech House, 2015, vol. 1.
- [17] Y. A. Thomas, "Linear quadratic optimal estimation and control with receding horizon," *Electronics Letters*, vol. 11, pp. 19–21, 1975.
- [18] B. K. Natarajan, "Sparse approximate solutions to linear systems," SIAM Journal on Computing, vol. 24, no. 2, pp. 227–234, 1995.
- [19] M. Kowalski, "Sparse regression using mixed norms," Applied and Computational Harmonic Analysis, vol. 27, no. 3, pp. 303–324, 2009.
- [20] H. Ohlsson, F. Gustafsson, L. Ljung, and S. Boyd, "Smoothed state estimates under abrupt changes using sum-of-norms regularization," *Automatica*, vol. 48, no. 4, pp. 595–605, 2012.
- [21] L. An and N. Sepehri, "Hydraulic actuator leakage fault detection using extended kalman filter," *International Journal of Fluid Power*, vol. 6, no. 1, pp. 41–51, 2005.